

Broadband control of the viscoelasticity of ferroelectrics via domain switching

C. S. Wojnar, J.-B. le Graverend, and D. M. Kochmann

Citation: [Applied Physics Letters](#) **105**, 162912 (2014); doi: 10.1063/1.4899055

View online: <http://dx.doi.org/10.1063/1.4899055>

View Table of Contents: <http://scitation.aip.org/content/aip/journal/apl/105/16?ver=pdfcov>

Published by the [AIP Publishing](#)

Articles you may be interested in

[Simulations of domain evolution in morphotropic ferroelectric ceramics under electromechanical loading using an optimization-based model](#)

[J. Appl. Phys.](#) **109**, 084107 (2011); 10.1063/1.3569583

[Domain switching mechanisms in polycrystalline ferroelectrics with asymmetric hysteretic behavior](#)

[J. Appl. Phys.](#) **105**, 024107 (2009); 10.1063/1.3068333

[Stress effects in sol-gel derived ferroelectric thin films](#)

[J. Appl. Phys.](#) **95**, 629 (2004); 10.1063/1.1632019

[Locking of electric-field-induced non-180° domain switching and phase transition in ferroelectric materials upon cyclic electric fatigue](#)

[Appl. Phys. Lett.](#) **83**, 3978 (2003); 10.1063/1.1626262

[Domain reorientation anisotropy in ferroelectric polycrystals](#)

[J. Appl. Phys.](#) **92**, 2112 (2002); 10.1063/1.1495531

The advertisement features a 3D cutaway of a mechanical part with a colorful stress or temperature distribution. The text 'Over 600 Multiphysics Simulation Projects' is prominently displayed in white and blue. A blue button with the text 'VIEW NOW >>' is located to the right. The COMSOL logo is in the bottom right corner.

Over **600** Multiphysics
Simulation Projects

[VIEW NOW >>](#)

COMSOL

Broadband control of the viscoelasticity of ferroelectrics via domain switching

C. S. Wojnar, J.-B. le Graverend, and D. M. Kochmann^{a)}

Graduate Aerospace Laboratories, California Institute of Technology, Pasadena, California 91125, USA

(Received 14 August 2014; accepted 10 October 2014; published online 24 October 2014)

We show that the viscoelastic properties of polycrystalline ferroelectric ceramics can be significantly altered over a wide range of mechanical frequencies when domain switching is controlled by cyclic electric fields. The dynamic stiffness of lead zirconate titanate is shown to vary by more than 30%, while damping increases by an order of magnitude. Experimental results are interpreted by the aid of a continuum-mechanics model that captures the nonlinear electro-mechanically coupled material response for the full electric hysteresis. © 2014 AIP Publishing LLC.

[<http://dx.doi.org/10.1063/1.4899055>]

Ferroelectric ceramics have been utilized to absorb vibrational energy primarily through the piezoelectric effect via Joule heating^{1,2} or by active control.³ These solutions provide significant damping over narrow frequency ranges while otherwise exhibiting little damping owing to the restricted material-inherent internal friction in metals and ceramics. Ferroelectricity provides for another, rather unexplored mechanism to dissipate mechanical energy, viz., the motion of domain walls, which may be induced by large mechanical stresses⁴ or electric fields⁵ (analogous to the motion of domain walls in ferromagnetic materials⁶). Besides the dissipation of electric energy visible in the hysteresis of electric displacement vs. electric field, we show that large electric fields can promote the mobility of domain walls to facilitate considerable dissipation in response to mechanical loads. The latter approach gives the tantalizing prospect of materials whose stiffness and damping can be dramatically changed by the push of a button. Current understanding is incomplete since previous studies were severely limited in the testable range of mechanical and electrical frequencies, and macroscopic models have not been developed to quantify the viscoelastic response of polycrystalline ferroelectrics under large bias electric fields. Domain wall kinetics have been explored before in single crystals; yet, the collective microstructural mechanisms in polycrystalline ceramics and the resulting electro-mechanically coupled macroscale behavior is far less understood.

We employ Broadband Electromechanical Spectroscopy (BES),⁷ which simultaneously applies electric fields and mechanical loads in a contactless fashion (see Fig. 1). Samples (38 mm long with a rectangular cross-section of $1 \times 3 \text{ mm}^2$) are tested in bending. A time-harmonic moment is applied via an attached permanent magnet placed between electromagnetic coils.⁸ Its relation to the specimen deflection (measured by a laser-detector setup) yields the dynamic stiffness $|E^*|$ and damping $\tan \delta = \text{Im } E^*/\text{Re } E^*$ (where E^* is the complex-valued Young modulus). Electric fields are applied via $10 \mu\text{m}$ thick Ni electrodes. Sinusoidal bending moments with frequencies ranging from 25 to 100 Hz and triangle waveforms of the bias electric field with frequencies ranging

from 0.01 to 1.0 Hz are simultaneously applied. Polarization changes are measured via a Sawyer-Tower circuit. The frequency of the bias electric field is chosen to be considerably lower than the mechanical frequency, which is sufficiently low to induce and affect domain wall motion, in particular, near the coercive field. In contrast to the equilibrium viscoelastic properties (measured, e.g., in single crystals at very low electric frequencies⁹), electric field rate dependence is present and worth exploring as a means of tuning the mechanical response. Experiments are performed under vacuum to remove spurious damping. Pure lead zirconate titanate (PZT) (Navy-type II; pre-poled and electroded) specimens with grain sizes around $2 \mu\text{m}$ have been tested. Fig. 2 illustrates the variations of stiffness and damping for four different electric field switching rates at a constant mechanical bending frequency. Consistent with previous findings for polycrystals,¹⁰ the coercive field increases with increasing electric frequency in the shown frequency range, cf. Fig. 2(a) (hysteresis asymmetry is a manufacturing artifact¹¹). Similar increases of the coercive field have been observed in PZN-PT single crystals.⁹

After the onset of domain switching (near the coercive field when the polarization is changing the most), the dynamic Young modulus softens significantly to below 70% of its original value without electric fields, see Fig. 2(b). The faster the electric cycling, the greater the softening effect. As observed in single-crystalline PZN-PT,¹² the modulus variation is partly due to elastic anisotropy: 90° -switched domains, observed in polycrystals under cyclic electric fields,¹³ reduce the apparent modulus in the loading direction. This effect is more gradual in polycrystals¹⁴ due to the

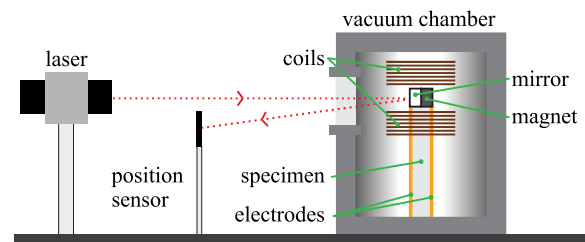


FIG. 1. Schematic view of the BES setup.

^{a)}Electronic mail: kochmann@caltech.edu

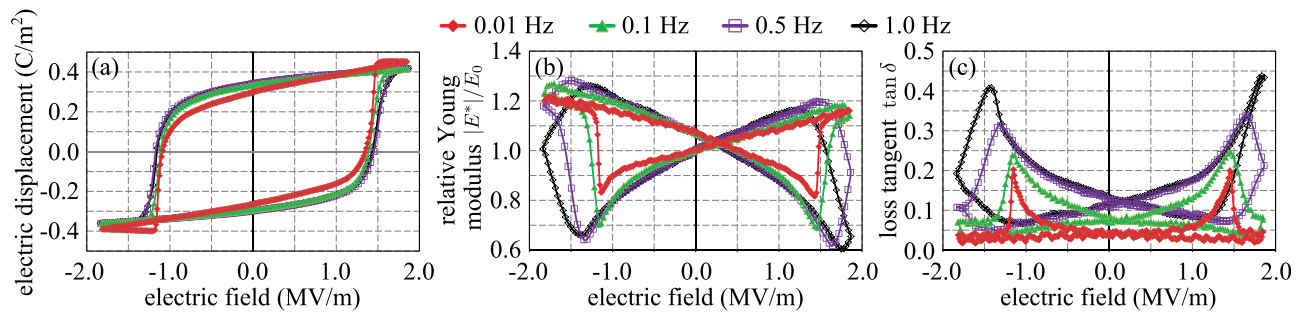


FIG. 2. Experimental data of (a) electric displacement, (b) relative Young modulus $|E^*/E_0|$ (with E_0 the modulus without electric bias), and (c) loss tangent $\tan \delta$ vs. electric field for triangle-wave electric field (1.8 MV/m amplitude) frequencies of 0.01, 0.1, 0.5, and 1.0 Hz and constant mechanical vibration at 75 Hz.

distributed grain orientations. Linear variation with electric field before and after switching was also observed in PZT polycrystals.¹⁵

The loss tangent shown in Fig. 2(c) exhibits peaks during domain switching, which become more pronounced with increasing electrical frequency. Like the dynamic Young modulus, the loss tangent varies linearly with the electric field before and after domain switching (as observed previously¹⁵). The remarkable damping seen during domain switching with $\tan \delta > 0.4$ is commonly found in polymers, rarely in ceramics. Its physical origin is similar to that found in single crystals¹² but the polycrystalline orientation distribution leads to a more gradual evolution of the macroscopic viscoelastic properties.

The rate-dependent stiffness and damping variations have been attributed to 90°-domain switching.^{4,16} For higher electrical frequencies, the domain wall velocity increases,^{17–19} which leads to an accelerated repoling process, see Fig. 2(a). This in turn results in larger spontaneous longitudinal strains during each mechanical cycle, thereby decreasing the apparent modulus. Also, the increases in domain wall velocity and apparent coercive field (which increases the domain wall driving force) jointly increase the dissipated energy. Owing to the analogous thermodynamic driving force arising from surfaces of discontinuities,²⁰ similar phenomena can be expected from domain wall motion in ferromagnetic materials.⁶

When keeping the electrical frequency constant at 0.1 Hz but changing the mechanical frequency, the polarization hysteresis curve remains unaffected (for the small moments applied), as shown in Fig. 3(a). Both the measured dynamic Young modulus and the loss tangent show small

variations with mechanical frequency, as shown in Figs. 3(b) and 3(c). Damping increases with frequency, and at high mechanical frequencies it is ultimately assisted by structural resonance of the specimen (occurring at 147 Hz under no electric field and decreasing during switching¹⁵ due to elastic modulus changes). Previous experiments showed a damping decrease over similar frequencies;⁵ however, those experiments were performed at elevated temperatures which are expected to decrease the relaxation time associated with domain switching. Higher mechanical frequencies are not presented here due to the difficulty of interpreting data near resonance. Experiments at ultrasonic frequencies (10 MHz) also revealed significant damping in single crystals;¹² yet, those primarily exploited the elastic anisotropy to be controlled by electric fields that affect the domain volume fractions. Here, the kinetic domain switching process itself produces remarkable variations in stiffness and damping.

There is a lack of electro-mechanically coupled models for polycrystalline ferroelectric ceramics that accurately describe the macroscopic dielectric and viscoelastic behavior for the full hysteresis. In the following, we outline a continuum model which does exactly this and thereby sheds light onto the evolution of the electric displacement, stiffness, and damping as observed in Figs. 2 and 3.

From the experimental geometry, we treat the specimen as a linear (visco)elastic Euler-Bernoulli beam; conditions well away from structural resonance admit using the correspondence principle.²¹ An electric field e is applied across the beam thickness, resulting in a macroscopic polarization p in the same direction (being accommodated by a mixture of differently polarized domains, and varying between $\pm p_s$, where p_s is the saturated polarization) and an axial strain

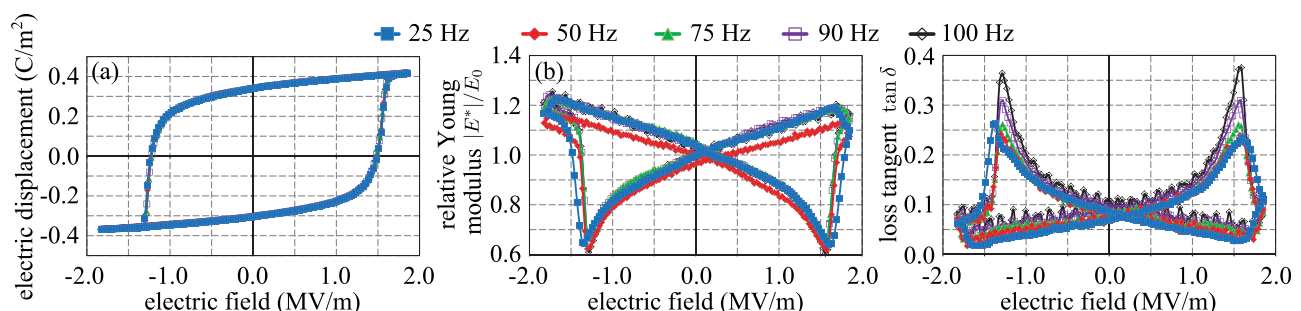


FIG. 3. Experimental data of (a) electric displacement, (b) relative Young modulus $|E^*/E_0|$, and (c) loss tangent $\tan \delta$ vs. electric field for mechanical frequencies of 25, 50, 75, 90, and 100 Hz and constant electric field cycling at 0.1 Hz.

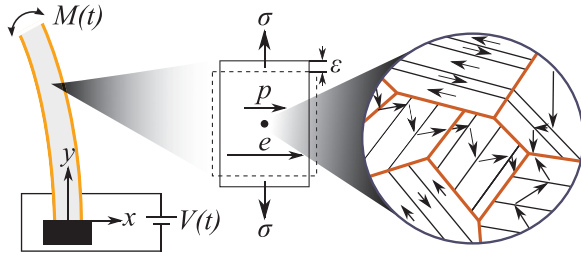


FIG. 4. Longitudinal stresses and transverse electric fields give rise to changes in the macroscopic polarization.

$-\varepsilon_s |p|/p_s$ with a corresponding spontaneous strain ε_s , as shown in Fig. 4. Onto this approximately quasistatically changing configuration, time-harmonic infinitesimal vibrations are imposed by an applied sinusoidal moment at the beam's free end, resulting in a total axial strain ε . We assume a variational constitutive law based on the stored energy $\psi(\varepsilon, e, p)$ with axial stress and electric displacement through the thickness given by $\sigma = \partial\psi/\partial\varepsilon$ and $d = -\partial\psi/\partial e$, respectively. The polarization evolution is governed by a kinetic relation $\dot{p} = f(y)$ with thermodynamic driving force $y = -\partial\psi/\partial p$ and dots denoting time derivatives.

To mimic experiments, stress, strain, and polarization are decomposed into their (quasistatic) averages plus spatial and time-varying perturbations

$$\begin{aligned}\sigma(x, y, t) &= \bar{\sigma} + \Delta\sigma(x, y, t), & \varepsilon(x, y, t) &= \bar{\varepsilon} + \Delta\varepsilon(x, y, t), \\ p(x, y, t) &= \bar{p} + \Delta p(x, y, t).\end{aligned}$$

Due to its slow variation relative to bending-induced perturbations, the applied electric field $e(t)$ is assumed constant. We expand the stress increment as

$$\begin{aligned}\Delta\sigma &= \sigma(\bar{\varepsilon} + \Delta\varepsilon, e, \bar{p} + \Delta p) - \sigma(\bar{\varepsilon}) \\ &= \frac{\partial^2\psi}{\partial\varepsilon^2}(\bar{\varepsilon})\Delta\varepsilon + \frac{\partial^2\psi}{\partial\varepsilon\partial p}(\bar{\varepsilon})\Delta p,\end{aligned}\quad (1)$$

where $(\bar{\varepsilon}) \equiv (\bar{\varepsilon}, e, \bar{p})$ abbreviates the average state (which we will drop in the sequel for brevity). The polarization increment is found by linearizing the kinetic relation

$$\Delta\dot{p} = \dot{p}(\bar{\varepsilon} + \Delta\varepsilon, e, \bar{p} + \Delta p) - \dot{p}(\bar{\varepsilon}) = \frac{\partial f}{\partial\varepsilon}\Delta\varepsilon + \frac{\partial f}{\partial p}\Delta p.\quad (2)$$

The polarization increment captures the rate dependence observed in experiments; application of a cyclic stress causes changes in the polarization, which tends to relax the stress, thereby reducing the modulus. Application of a time-harmonic bending moment with frequency ω (neglecting transient effects), results in stress, strain, and polarization increments at the same frequency, so that $\Delta p(x, y, t) = \Delta p(x, y) e^{i\omega t}$. Substituting into (2) yields

$$\Delta p = \frac{\partial f}{\partial\varepsilon}\Delta\varepsilon \Big/ \left(i\omega - \frac{\partial f}{\partial p} \right).\quad (3)$$

Inserting Eq. (3) into Eq. (1) and noting that $\Delta\sigma = E^*\Delta\varepsilon$, we arrive at the complex-valued Young modulus

$$E^* = E_0 - \frac{\partial f}{\partial\varepsilon} \frac{\partial y}{\partial\varepsilon} \Big/ \left(i\omega - \frac{\partial f}{\partial p} \right),\quad (4)$$

where $E_0^* = \partial^2\psi/\partial\varepsilon^2$ represents the material's base Young modulus. The dynamic viscoelastic Young modulus and loss tangent thus follow as,²¹ respectively,

$$|E^*| = \sqrt{\text{Re}(E^*)^2 + \text{Im}(E^*)^2}, \quad \tan\delta = \frac{\text{Im}(E^*)}{\text{Re}(E^*)}.\quad (5)$$

The \bar{p} - e hysteresis is obtained by integrating the kinetic relation. To evaluate Eq. (5) given a point (e, \bar{p}) on the \bar{p} - e loop, the strain $\bar{\varepsilon}$ is computed by enforcing $\bar{\sigma}(\bar{\varepsilon}, e, \bar{p}) = 0$.

For ferroelectrics, the stored energy density for the cantilever beam in pure bending is taken as

$$\begin{aligned}\psi &= \frac{E_0^*(e, p, \omega)}{2} [\varepsilon - \varepsilon^r(p)]^2 - \frac{\varepsilon}{2} e^2 - e p + \psi^{\text{rem}}(p) \\ &\text{with } \psi^{\text{rem}}(p) = -h[\log(1 - |p|/p_s) + |p|/p_s] \\ E_0^*(e, p, \omega) &= E'(e, p) [1 + i \tan\delta(e, p, \omega)],\end{aligned}$$

where $\varepsilon^r = -\varepsilon_s |p|/p_s$ is the net axial polarization strain due to 90°-domain switching, and ε is the electric permittivity. ψ^{rem} is the relaxed polarization energy.²² A commonly used kinetic relation is $\dot{p} = \langle |y|/e_c - 1 \rangle^m \text{sign}(y)/\eta$, i.e., domain switching occurs at a rate depending on m and viscosity η when the driving force exceeds the coercive field e_c . Based on experimental observations, the complex Young modulus $E_0^* = E'(1 + i \tan\delta)$ is defined by

$$\begin{aligned}E' &= E_0 [1 + c_1 e p / (e_c p_s) + c_2 |p|/p_s], \\ \tan\delta &= \tan\delta_0 + c_3 e p / (e_c p_s) + c_4 \omega [1 - (p/p_s)^2]^2.\end{aligned}$$

Constant c_1 characterizes the approximately linear variation of the Young modulus with electric field and constant c_2 characterizes the polarization dependence (due to anisotropy). The loss tangent depends linearly on the electric bias through c_3 and on the mechanical frequency through c_4 ; the latter dependence peaks during domain switching (experimentally observed near $\bar{p} = 0$). E_0 and $\tan\delta_0$ are, respectively, the Young modulus and loss tangent without an applied electric field. Experiments show no variation in the electric displacement with ω . Thus, the increasing loss tangent with mechanical frequency is included in the complex modulus instead of the kinetic relation (microscale oscillations of domain walls would not be captured in the evolution of the macroscopic polarization). Material parameters (unless known from the supplier) were obtained by fitting experimental data (see Table I).

The model predictions shown in Fig. 5 agree well with the experimental data in Figs. 2 and 3. We see qualitatively the same behavior: linear variations of stiffness and damping with electric field away from domain switching as well as

TABLE I. Material parameters for polycrystalline PZT.

Parameter	Known value	Parameter	Fitted value
E_0	66 GPa	η	0.002 m ² s/C
$\tan\delta_0$	0.08	m	2
ε	41×10^{-9} J/(mV ²)	c_1	0.25
p_s	0.37 C/m ²	c_2	0.5
ε_s	0.001	c_3	-0.03
e_c	1.2 MV/m	c_4	4.2×10^{-4} s
		h	3×10^4 J/m ³

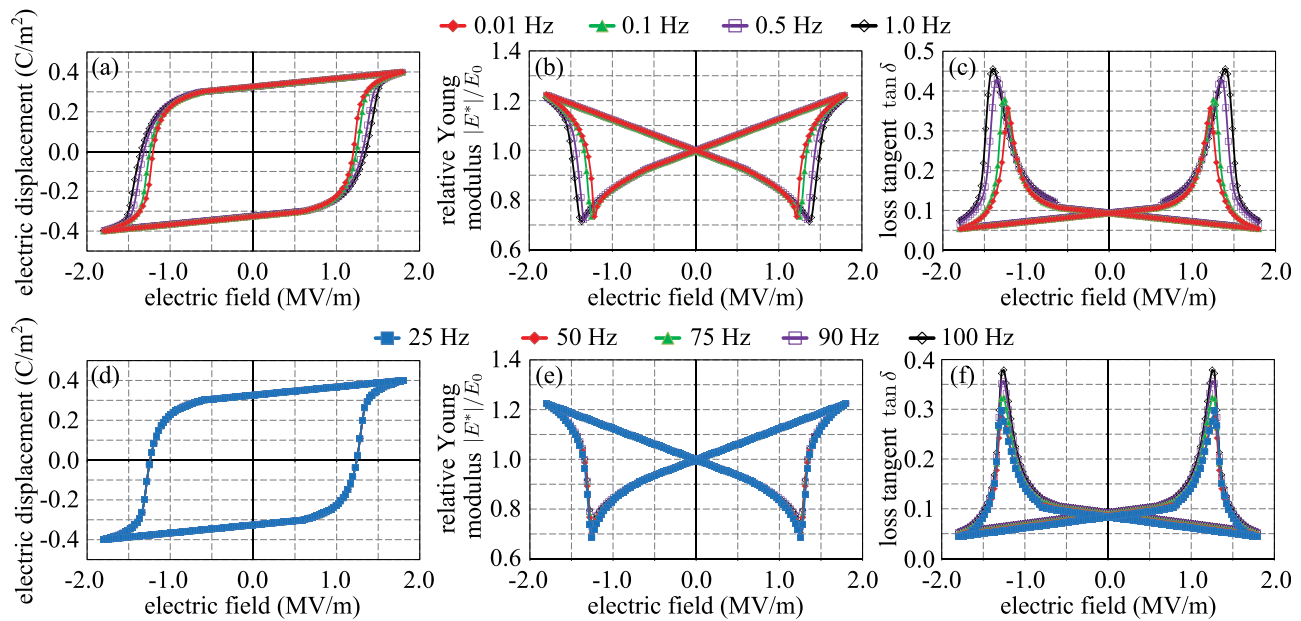


FIG. 5. (a–c) and (d–f) show the simulated results for the same conditions as experiments in Fig. 2 and Fig. 3, respectively.

pronounced softening and damping during domain switching that increase with electric frequency. The model also captures an increase of the damping peaks during domain switching with increasing mechanical frequency. Decreasing the viscosity η , increasing the spontaneous strain ε_s , or increasing the modulus E_0 promotes higher damping and stronger softening during switching.

We have shown how 90° -domain switching in ferroelectrics (induced by a large, cyclically changing electric field) leads to significant changes of the material's dynamic stiffness and damping and is controllable via the electrical and mechanical loading frequencies. The phenomenon has been demonstrated experimentally for a range of mechanical frequencies and has been explained by a phenomenological macroscale model for polycrystalline ferroelectrics. Broadband controllability of damping and stiffness, particularly of stiff materials, is of importance for scientific and technological applications including seismic insulation, control of acoustic and mechanical vibrations, sensors, wave guides, and filters.

We thank Kaushik Bhattacharya for many fruitful discussions. We acknowledge support from United Technologies Research Center and Caltech's Innovation Initiative.

- ¹N. Hagood and A. von Flotow, *J. Sound Vib.* **146**, 243 (1991).
- ²T. Asare, B. Poquette, J. Schultz, and S. Kampe, *J. Mater. Sci.* **47**, 2573 (2012).
- ³L. Zheng, D. Zhang, and Y. Wang, *Smart Mater. Struct.* **20**, 025008 (2011).
- ⁴P. M. Chaplya and G. P. Carman, *J. Appl. Phys.* **92**, 1504 (2002).
- ⁵B. Jiménez and J. Vicente, *J. Phys. D* **33**, 1525 (2000).
- ⁶M. Wuttig, Q. Su, F. Masson, E. Quandt, and A. Ludwig, *J. Appl. Phys.* **83**, 7264 (1998).
- ⁷J.-B. le Graverend, C. S. Wojnar, and D. M. Kochmann, "Broadband Electromechanical Spectroscopy (BES): Measuring the dynamic mechanical response of viscoelastic materials under temperature and electric-field control in a vacuum environment" (unpublished).
- ⁸C. P. Chen and R. S. Lakes, *J. of Rheology* **33**(8), 1231 (1989).
- ⁹J. Yin and W. Cao, *Appl. Phys. Lett.* **80**, 1043 (2002).
- ¹⁰D. Zhou, M. Kamlah, and D. Munz, *J. Am. Ceram. Soc.* **88**, 867 (2005).
- ¹¹K. Carl and K. Härdtl, *Ferroelectrics* **17**, 473 (1978).
- ¹²J. Yin and W. Cao, *Appl. Phys. Lett.* **79**, 4556 (2001).
- ¹³T. Tsurumi, Y. Kumano, N. Ohashi, T. Takenaka, and O. Fukunaga, *Jpn. J. Appl. Phys., Part 1* **36**, 5970 (1997).
- ¹⁴S. R. Burlage, *IEEE Trans. Sonics Ultrason.* **12**, 5 (1965).
- ¹⁵Q.-M. Wang, T. Zhang, Q. Chen, and X.-H. Du, *Sens. Actuators, A* **109**, 149 (2003).
- ¹⁶G. Arlt and H. Dederichs, *Ferroelectrics* **29**, 47 (1980).
- ¹⁷W. J. Merz, *J. Appl. Phys.* **27**, 938 (1956).
- ¹⁸R. Müller and A. Savage, *Phys. Rev.* **112**, 755 (1958).
- ¹⁹G. Tatara and H. Kohno, *Phys. Rev. Lett.* **92**, 086601 (2004).
- ²⁰R. Abeyaratne and J. K. Knowles, *J. Mech. Phys. Solids* **38**, 345 (1990).
- ²¹R. Lakes, *Viscoelastic Solids* (CRC Press, 1999).
- ²²C. Miehe and D. Rosato, *Int. J. Eng. Sci.* **49**, 466 (2011).